PAPER K

FBI FOR FIELD CONTINUITY AT INTERIOR INTERFACES FOR WAVES IN HETEROGENEOUS MEDIA

Zhongjie Zhang*, Youli Quan, Xiaofei Chen, and Jerry M. Harris

ABSTRACT

It is difficult to locate the position of an interior interface, to describe the elastic properties above and below an interior interface when the conventional finite difference method is used to simulate the seismic wave-field in complex media. Generally, the interior interface is treated as a transition zone, the fidelity of seismic behavior on the interface would not be permitted. In this paper, an algorithm, referred as Forward-Backward Iteration (FBI) technique is developed to keep the continuity condition valid at each node on the interior interface. It looks to be the repeatedly weighed average of the wave-field above and underneath the interface node in the condition of meeting the requirements of the continuity condition at the node, but different from the weighed average in the conventional meaning. The treatment of continuity is taken node by node when the node is on the interior interface, which permits the algorithm can be adapted to heterogeneous, anisotropic media with complicated structure. The model computation shows that the algorithm is stable and feasible, and requires little additional computer memory.

* Institute of Geophysics, Chinese Academy of Sciences, China

INTRODUCTION

Finite difference methods are widely used to numerically simulate acoustic and elastic wave-fields in inhomogeneous isotropic and anisotropic media. Many different finite difference schemes have been developed, for example, Tsingas et al. (1990) presented a modelling algorithm which uses finite difference operators for the solution of differential equations that describe wave propagation in transversely isotropic media, Faria et al. (1994) presented a 2-D finite difference method for modelling seismic propagation in a transversely isotropic media based on the staggered grid scheme (Vireux, 1986; Levander, 1988).

Except for the treatments of artificial boundaries, stability of algorithm, grid dispersion, and source distribution, the treatment of interior interfaces is also necessary, because the codes of finite difference algorithm can be used on all grid points except the boundaries of the computational region. to get a highly precisive modelling method. In most schemes for compute the wave-fields in heterogeneous media, the material parameters are represented by their actual local values or by arithmetic averages from neighboring grid points (Kelly et al., 1976; Stephen, 1983; Baileys et al., 1986; Viriveux, 1986; Levander, 1988; Sochachi, et al., 1991), some researchers have used the effective parameters, that is, the actual variations between the grid points are approximated by certain integral averages (Boore, 1972; Kummer and Bahle, 1982; Zahradnik, 1985, 1990; Kummer, et al., 1987; Zahrednik and Horn, 1987; Moczo, 1989). It works reasonably well for relatively coarse grids and flat interfaces but does not automatically predict the correct behavior at elastic discontinuities with complicate geometrical features. Generally, the discontinuity interface is treated as an artificial transition zone. But few studies have been done on the problem of the interior interface with finite difference methods in heterogeneous anisotropic media.

In this paper, we first analyze the disadvantages of conventional finite difference methods for the node at the interior interface, then we will study the FBI technique in 2D heterogeneous, transversely isotropic media with a curved interface, and finally, we will implement the modelling of multi-component seismic wave-fields in isotropic and anisotropic media. The results show the scheme is stable for complicated structure and media and can be easily extended to 3D problems.

ANALYSIS OF CONTINUITY CONDITION AT INTERIOR INTERFACE

As we just interest in the seismic propagation when the interior interface is met, so we can now consider the case of seismic propagation without the terms of forces. We know, in

2D inhomogeneous transversely isotropic media, the wave equations could be written as follows:

$$\rho(x,z)\frac{\partial^2}{\partial t^2}\boldsymbol{u}(x,z,t)=\frac{\partial}{\partial x}\left[\boldsymbol{B}(x,z)\frac{\partial}{\partial x}\boldsymbol{u}(x,z,t)\right]+\frac{\partial}{\partial x}\left[\boldsymbol{D}(x,z)\frac{\partial}{\partial z}\boldsymbol{u}(x,z,t)\right]$$
$$+\frac{\partial}{\partial z}\left[\boldsymbol{E}(x,z)\frac{\partial}{\partial x}\boldsymbol{u}(x,z,t)\right]+\frac{\partial}{\partial z}\left[\boldsymbol{G}(x,z)\frac{\partial}{\partial z}\boldsymbol{u}(x,z,t)\right], \tag{1}$$

where $\boldsymbol{u}(x,z,t)=[u_x,u_y,u_z]^T$ is the displacement vector, and $u_x(x,z,t),u_y(x,z,t),u_z(x,z,t)$ are the displacement components in x , y and z-directions, respectively. $\rho(x,z)$ is the density of media and x, z, t, are space and time coordinates. Matrices $\boldsymbol{B}$, $\boldsymbol{D}$, $\boldsymbol{E}$ and $\boldsymbol{G}$ are written in the following forms:

$$\boldsymbol{B}(x,z)=\begin{bmatrix}C_{11}(x,z) & C_{15}(x,z) & C_{16}(x,z)\\ C_{15}(x,z) & C_{55}(x,z) & C_{56}(x,z)\\ C_{16}(x,z) & C_{56}(x,z) & C_{66}(x,z)\end{bmatrix}\qquad \boldsymbol{D}(x,z)=\begin{bmatrix}C_{15}(x,z) & C_{13}(x,z) & C_{14}(x,z)\\ C_{55}(x,z) & C_{35}(x,z) & C_{45}(x,z)\\ C_{66}(x,z) & C_{36}(x,z) & C_{46}(x,z)\end{bmatrix}$$

$$\boldsymbol{E}(x,z)=\begin{bmatrix}C_{15}(x,z) & C_{55}(x,z) & C_{56}(x,z)\\ C_{13}(x,z) & C_{35}(x,z) & C_{36}(x,z)\\ C_{14}(x,z) & C_{45}(x,z) & C_{46}(x,z)\end{bmatrix}\qquad \boldsymbol{G}(x,z)=\begin{bmatrix}C_{55}(x,z) & C_{35}(x,z) & C_{45}(x,z)\\ C_{35}(x,z) & C_{33}(x,z) & C_{34}(x,z)\\ C_{45}(x,z) & C_{34}(x,z) & C_{44}(x,z)\end{bmatrix}$$

Where, c_{ij} (x, z) (i, j=1, 2,...6) is elastic parameter of anisotropic media.

Eq. (1) can be solved with a numerical discretization technique. The discretized finite difference forms of Eq. (1) can be written as :

$$\boldsymbol{U}(i,j,n+1)=2\boldsymbol{U}(i,j,n)-\boldsymbol{U}(i,j,n-1)$$
$$+\frac{(\Delta t)^2}{\rho_{ij}(\Delta x)^2}\left\{B(i+\frac{1}{2},j)[U(i+1,j,n)-U(i,j,n)]-B(i-\frac{1}{2},j)[U(i,j,n)-U(i-1,j,n)]\right\}$$
$$+\frac{(\Delta t)^2}{\rho_{ij}(\Delta x\Delta z)}\{D(i+1,j)[U(i+1,j+1,n)-U(i+1,j-1,n)]$$
$$-D(i-1,j)[U(i-1,j+1,n)-U(i-1,j-1,n)]$$

$$+E(i,j+1)[U(i+1,j+1,n)-U(i-1,j+1,n)]-E(i,j-1)[U(i+1,j-1,n)-U(i-1,j-1,n)]\}$$

$$+\frac{(\Delta t)^2}{\rho_{ij}(\Delta z)^2}\left\{G(i,j+\frac{1}{2})[U(i,j+1,n)-U(i,j,n)]-G(i,j-\frac{1}{2})[U(i,j,n)-U(i,j-1,\Delta n)]\right\} \quad (2)$$

where, $U(i,j,n)=\boldsymbol{u}(i\Delta x, j\Delta z, n\Delta t)$, Δx, Δz, Δt are the discretized decrements for the spatial coordinate x and z, and time t. An interior interface R is illustrated in Fig. 1, and can be described by a bi-cubic, spline, interpolation technique. The elastic parameters above and underneath the interface R can also be interpolated by bi-cubic spline functions. When we consider only the transversely isotropic media, the elastic parameters of the two media which is separated by the discontinuity surface R are denoted as: $C_{11}(i,j)$ $C_{13}(i,j)$, $C_{33}(i,j)$ $C_{44}(i,j)$, $C_{66}(i,j)$ and $C_{11}(i,j+\varepsilon)$, $C_{13}(i,j+\varepsilon)$, $C_{33}(i,j+\varepsilon)$, $C_{44}(i,j+\varepsilon)$, $C_{66}(i,j+\varepsilon)$,. In order to analyze the condition of continuity at the interior interface R, we choose a given point (i,j) on the interface R and minimum quantity variation ε in the direction of the z-axis. By taking a Taylor expansion of Eq. (2) at the point (i, j), we can get the following equations when we consider only ux and uz components here and when ε=0:

$$\frac{C_{44}(i,j)+C_{44}(i,j+\varepsilon)}{2}\frac{\partial u_x(i,j+\varepsilon)}{\partial z}+\frac{C_{13}(i,j+\varepsilon)+C_{44}(i,j)}{2}\frac{\partial u_z(i,j+\varepsilon)}{\partial x}=$$
$$C_{44}(i,j)\frac{\partial u_x(i,j)}{\partial z}+\frac{C_{13}(i,j)+C_{44}(i,j)}{2}\frac{\partial u_z(i,j)}{\partial x} \quad (3a)$$

and:

$$\frac{C_{33}(i,j)+C_{33}(i,j+\varepsilon)}{2}\frac{\partial u_z(i,j+\varepsilon)}{\partial z}+\frac{C_{13}(i,j+\varepsilon)+C_{44}(i,j)}{2}\frac{\partial u_x(i,j+\varepsilon)}{\partial x}=$$
$$C_{33}(i,j)\frac{\partial u_z(i,j)}{\partial z}+\frac{C_{13}(i,j)+C_{44}(i,j)}{2}\frac{\partial u_x(i,j)}{\partial x} \quad (3b)$$

Obviously, the condition of stress continuity on the interface is not exactly satisfied even if the interior interface is considered as a flat discontinuity . Even though there are some difference of the finite difference formula from each researcher, the invalidity of stress continuity condition at the discontinuity always exists more or less. It is more serious when the surface of discontinuity is not flat, but roughly curved without special treatment at each node on the inner interface. Meanwhile, it is difficult to determine what kind of elastic parameters should be set for the node on the interface. if the average elastic parameters are given, the discontinuity would be smoothed. In the next section, we will introduce one way to treat these kinds of problems.

WAVEFIELDS' EXPRESSION AT INTERIOR INTERFACE IN HETEROGENEOUS MEDIA

For the curved interface illustrated in Fig. 1, which can be approached by bi-cubic spline interpolation, the elastic parameters (in anisotropic media) or velocities (in isotropic media) just above or underneath the curved interface can also be described by spline interpolation. In this way, we can locate the interface, and determine the elastic property of the media separated by the interface more clearly and accurately.

We will arbitrarily choose one point A(i, j) on the interface R. The angle between the normal direction and the vertical z-axis is denoted as θ, which can be calculated automatically in the process of interpolation of the geometry parameter of the interior interface R. By using the coordinate transformation, the condition of stress continuity at point A on the interface R could be written in the following forms for ux and uz component computation:

$$\sigma_{zz}^{a}\sin\theta+\sigma_{xz}^{a}\cos\theta=\sigma_{zz}^{b}\sin\theta+\sigma_{xz}^{b}\cos\theta \tag{4a}$$

and

$$\sigma_{zz}^{a}\cos\theta-\sigma_{xz}^{a}\sin\theta=\sigma_{zz}^{b}\cos\theta-\sigma_{xz}^{b}\sin\theta \tag{4b}$$

Where, σ_{zz}^{a}, σ_{xz}^{a}, σ_{zz}^{b}, and σ_{xz}^{b} are the normal and shear stress components for the media above and underneath (below) the interface R, respectively.

When we consider the seismic waves in transversely isotropic media here, the elastic parameters at the interface node A(i, j) just above and below the interface are defined as: $C_{11}^{a}(i,j), C_{13}^{a}(i,j), C_{33}^{a}(i,j), C_{44}^{a}(i,j), C_{66}^{a}(i,j)$, $C_{11}^{b}(i,j), C_{13}^{b}(i,j), C_{33}^{b}(i,j), C_{44}^{b}(i,j), C_{66}^{b}(i,j)$ respectively. So the relations between the stress components σ_{zz}^{a}, σ_{xz}^{a}, σ_{zz}^{b}, and σ_{xz}^{b} and the displacement components above and underneath the interface R are:

$$\sigma_{zz}^{a}=C_{13}^{a}\frac{\partial u_{x}^{a}}{\partial x}+C_{33}^{a}\frac{\partial u_{z}^{a}}{\partial z} \tag{5a}$$

$$\sigma_{zz}^{b}=C_{13}^{b}\frac{\partial u_{x}^{b}}{\partial x}+C_{33}^{b}\frac{\partial u_{z}^{b}}{\partial z} \tag{5b}$$

and

$$\sigma_{xz}^{a}=C_{44}^{a}\left(\frac{\partial u_{x}^{a}}{\partial z}+\frac{\partial u_{z}^{a}}{\partial x}\right) \tag{5c}$$

$$\sigma_{xz}^{b} = C_{44}^{b}\left(\frac{\partial u_x^b}{\partial z} + \frac{\partial u_z^b}{\partial x}\right) \tag{5d}$$

Combining Eq. (4a), (4b) and (5a-5d), and discretizing the conditions of stress continuity with the finite difference method, we can obtain the relationships between the wave-fields Ux and Uz at the interface node and the wave-fields at the related nodes which are above and underneath the given interface node in the following form:

$$\begin{bmatrix} U_x(i,j,n) \\ U_z(i,j,n) \end{bmatrix} = \begin{bmatrix} a_{11} & a_{12} \\ a_{21} & a_{22} \end{bmatrix}^{-1} \begin{bmatrix} b_1 \\ b_2 \end{bmatrix} \tag{6}$$

Where the elements a_{11}, a_{12}, a_{21}, a_{22}, b_1, b_2 of the above matrix are:

$$a_{11} = \frac{C_{13}^a + C_{13}^b}{\Delta x}\cos\theta - \frac{C_{44}^a + C_{44}^b}{\Delta z}\sin\theta \qquad a_{12} = \frac{C_{33}^a + C_{33}^b}{\Delta z}\cos\theta - \frac{C_{44}^a + C_{44}^b}{\Delta x}\sin\theta$$

$$a_{21} = \frac{C_{13}^a + C_{13}^b}{\Delta x}\sin\theta + \frac{C_{44}^a + C_{44}^b}{\Delta z}\cos\theta \qquad a_{22} = \frac{C_{33}^a + C_{33}^b}{\Delta z}\sin\theta + \frac{C_{44}^a + C_{44}^b}{\Delta x}\cos\theta$$

$$b_1 = \left(\frac{C_{13}^b}{\Delta x}U_x(i+1,j,n) + \frac{C_{13}^a}{\Delta x}U_x(i-1,j,n) + \frac{C_{33}^b}{\Delta z}U_z(i,j+1) + \frac{C_{33}^a}{\Delta z}U_z(i,j-1)\right)\cos\theta$$
$$-\left(\frac{C_{44}^b}{\Delta z}U_x(i,j+1) + \frac{C_{44}^a}{\Delta z}U_x(i,j-1) + \frac{C_{44}^b}{\Delta x}U_z(i+1,j) + \frac{C_{44}^a}{\Delta x}U_z(i-1,j)\right)\sin\theta$$

$$b_2 = \left(\frac{C_{13}^b}{\Delta x}U_x(i+1,j) + \frac{C_{13}^a}{\Delta x}U_x(i-1,j) + \frac{C_{33}^b}{\Delta z}U_z(i,j+1) + \frac{C_{33}^a}{\Delta z}U_z(i,j-1)\right)\sin\theta$$
$$+\left(\frac{C_{44}^b}{\Delta z}U_x(i,j+1) + \frac{C_{44}^a}{\Delta z}U_x(i,j-1) + \frac{C_{44}^b}{\Delta x}U_z(i+1,j) + \frac{C_{44}^a}{\Delta x}U_z(i-1,j)\right)\cos\theta$$

Similiary, we can use the condition of stress continuity, and get the relationship between the wavefield of Uy component at the interface node A(i, j) and that above and below the node A(i, j) in the following form:

$$U_y(i,j,n) = \frac{C_{44}^b U_y(i,j+1,n) + C_{44}^a U_y(i,j-1,n)}{C_{44}^a + C_{44}^b} \tag{7}$$

When the interface is flat and even, we have the same form of relationship Eq. (6), but the elements a_{ij} and b_i $(i, j=1,2)$ would be:

$$a_{11} = \frac{C_{13}^a + C_{13}^b}{\Delta x} \qquad a_{12} = \frac{C_{33}^a + C_{33}^b}{\Delta z}$$

$$a_{21} = \frac{C_{44}^a + C_{44}^b}{\Delta z} \qquad a_{22} = \frac{C_{44}^a + C_{44}^b}{\Delta x}$$

$$b_1 = \frac{C_{13}^b}{\Delta x} U_x(i+1,j) + \frac{C_{13}^a}{\Delta x} U_x(i-1,j) + \frac{C_{33}^b}{\Delta z} U_z(i,j+1) + \frac{C_{33}^a}{\Delta z} U_z(i,j-1)$$

$$b_2 = \frac{C_{44}^b}{\Delta x} U_z(i+1,j) + \frac{C_{44}^a}{\Delta x} U_z(i-1,j) + \frac{C_{44}^b}{\Delta z} U_x(i,j+1) + \frac{C_{44}^a}{\Delta z} U_x(i,j-1)$$

When there is a segment of vertical fault in the computational region of the model, we will have:

$$a_{11} = -\frac{C_{44}^a + C_{44}^b}{\Delta z} \qquad a_{12} = -\frac{C_{44}^a + C_{44}^b}{\Delta x}$$

$$a_{21} = \frac{C_{13}^a + C_{13}^b}{\Delta x} \qquad a_{22} = \frac{C_{33}^a + C_{33}^b}{\Delta z}$$

$$b_1 = -\left(\frac{C_{44}^b}{\Delta x} U_z(i+1,j) + \frac{C_{44}^a}{\Delta x} U_z(i-1,j) + \frac{C_{44}^b}{\Delta x} U_z(i+1,j) + \frac{C_{44}^a}{\Delta x} U_z(i-1,j) \right)$$

$$b_2 = \left(\frac{C_{13}^b}{\Delta x} U_x(i+1,j) + \frac{C_{13}^a}{\Delta x} U_x(i-1,j) + \frac{C_{33}^b}{\Delta z} U_z(i,j+1) + \frac{C_{33}^a}{\Delta z} U_z(i,j-1) \right)$$

Where, the relationship about the wave-field Uy at the interface node is the same as Eq. (9).

When the media are simplified and become inhomgeneous and isotropic, then the wave-fields Ux, Uz and Uy at the interface node would be:

$$a_{11} = \rho\left(\frac{V_{pa}^2 + V_{pb}^2 - V_{sa}^2 - V_{sb}^2}{\Delta x} \cos\theta - \frac{V_{sa}^2 + V_{sb}^2}{\Delta z} \sin\theta \right) \qquad a_{12} = \rho\left(\frac{V_{pa}^2 + V_{pb}^2}{\Delta z} \cos\theta - \frac{V_{sa}^2 + V_{sb}^2}{\Delta x} \sin\theta \right)$$

$$a_{21} = \rho\left(\frac{V_{pa}^2 + V_{pb}^2 - V_{sa}^2 - V_{sb}^2}{\Delta x} \sin\theta + \frac{V_{sa}^2 + V_{sb}^2}{\Delta z} \cos\theta \right) \qquad a_{22} = \rho\left(\frac{V_{pa}^2 + V_{pb}^2}{\Delta z} \sin\theta + \frac{V_{sa}^2 + V_{sb}^2}{\Delta x} \cos\theta \right)$$

$$b_1 = \rho \left(\frac{V_{pb}^2}{\Delta x} U_x(i+1,j,n) + \frac{V_{pa}^2}{\Delta x} U_x(i-1,j,n) + \frac{V_{pb}^2}{\Delta z} U_x(i,j+1,n) + \frac{V_{pa}^2}{\Delta z} U_x(i,j-1,n) \right) \cos\theta$$

$$- \left(\frac{V_{pb}^2}{\Delta x} U_x(i+1,j,n) + \frac{V_{pa}^2}{\Delta x} U_x(i-1,j,n) + \frac{V_{pb}^2}{\Delta z} U_x(i,j+1,n) + \frac{V_{pa}^2}{\Delta z} U_x(i,j-1,n) \sin\theta \right.$$

$$b_2 = \rho \left(\frac{V_{pb}^2}{\Delta x} U_x(i+1,j,n) + \frac{V_{pa}^2}{\Delta x} U_x(i-1,j,n) + \frac{V_{pb}^2}{\Delta z} U_x(i,j+1,n) + \frac{V_{pa}^2}{\Delta z} U_x(i,j-1,n) \sin\theta \right.$$

$$+ \left(\frac{V_{pb}^2}{\Delta x} U_x(i+1,j,n) + \frac{V_{pa}^2}{\Delta x} U_x(i-1,j,n) + \frac{V_{pb}^2}{\Delta z} U_x(i,j+1,n) + \frac{V_{pa}^2}{\Delta z} U_x(i,j-1,n) \cos\theta \right.$$

The wavefields of y-component can be described as:

$$U_y(i,j,n) = \frac{V_{sb}^2 U_y(i,j+1,n) + V_{sa}^2 U_y(i,j-1,n)}{V_{sa}^2 + V_{sb}^2}$$

Where, Vpb, Vpa, Vsb and Vsa are the P-wave and S-wave velocity below and above the interface node respectively.

We can see from the above expressions, the wave-fields Ux, Uy and Uz at the interface node connect with the waffled just above and below the interface. In the next section, wewill use such a phenomenon and adapt Forward-Backward Iteration technique to make the condition of stress continuity satisfied.

FBI TECHNIQUE AT DISCONTINUITY AND IT'S IMPLEMENTATION

In the process of computing acoustic or elastic wave-fields, we can check whether the node under computation intersects the interface or not. If the node meets one interface, we can proceed to the next node in the vertical or horizontal direction . In such a way, we can get the initial value for iteration (namely, 0th order approximation of the wave-fields dt the interface node and the neighboring node (underneath the interface)). Then, we can get the modified wave-fields (namely, the 1st approximation of wave-fields at the interface node) at the interface node with the 0th approximating values at the interface node and the neighboring nodes just above and underneath the interface node. Using the modified values at the interface node, the wave-fields underneath the interface node can be obtained with the conventional finite difference method, repeat this process, the wave-fields at the interface node can be modified iteratively many times to approach the real effect of interior interface.

This process can be illustrated by Fig. 2. The flowcharts of Fig. 3a and 3b give an interpretation of a one-time iteration for Uy, Ux and Uz component computation respectively. The most important element in this process is the weighted average of wave-fields for the nodes above and below (for non vertical discontinuity), right and left (for vertical discontinuity) of the interface satisfying the condition of stress continuity at each node on each interior interface and the locations. The physical property of the media separated by the complex discontinuity can then be more accurately determined. The iteration times can be chosen according by the requirements of the problem being solved.

COMPUTATION

Synthetical computations were made for two models; Model 1 corresponds to two-layer isotropic media, Model 2 corresponds to two-layer transversely isotropic media. Figure 4a-c, and 5a-c are snapshots of the Ux, Uy and Uz components for two-layer isotropic model with and without FBI treatment of stress continuity at the interior interface, Figure 6a-c, and 7a-c are snapshots for two transversely isotropic model with and without FBI treatment of the interior interface.

CONCLUSION

We have presented the FBI technique for the treatment of stress continuity at the interior interface for heterogeneous transversely isotropic media. The position of the interior interface and the elastic property for media separated by the interior interface can be approached by the bi-cubic spline interpolation method out of consideration of the transition zone for the interior interface. This algorithm can be extended easily to 3-D and other kinds of complicated media and structure.

ACKNOWLEDGMENTS

The first author would like to thank the Chinese Nature Science Foundation, the President's Foundation of the Chinese Academy of Sciences for their support of this research.

REFERENCE

Bayliss, A. , Jordan K. E., Lemesurier B. J., and Turkel E., 1986, A fourth-order accurate finite-difference scheme for the computation of elastic wave, Bull. Seis. Soc. Am., **76**, 1115-1132.

Boore, D. M. , 1972, Finite-difference methods for seismic waves, In methods in computational physics, B. A. Bolt (Editor), Academic Press, New York, **11**, 1-37.

Eduardo L. Faria and Stoffa Paul L., 1994, Finite-difference modelling in transversely isotropic media, Geophysics, **59**, 282-289.

Igel H., Mora P., and Riollet B., 1993, Anisotropic wave propagation through finite-difference grids, Canadian Journal of Exploration Geophysics, 29, 59-77.

Kelly, K. R. , Ward, R. W. , et al. , 1976, Synthetic seismograms: a finite-difference approach, Geophysics, **41**, 2-27.

Kummer, B. , Behle A., and Dorau F., 1987, Hybrid modelling of elastic wave propagation in two-dimensional laterally inhomgeneous media, Geophysics, **52**, 765-771.

Kummer, B. and Bahle, B. , 1982, Second-order finite-difference modelling of SH-wave propagation in laterally inhomogeneous media, Bull. Seis. Soc. Am. , **72**, 793-808.

Levander, A. R. , 1988, Fourth-order finite-difference P-SV seismogram, Geophysics, **53**, 1425-1436.

Moczo, P. , 1989, Finite-difference technique for SH-wave in 2-D media using irregular grids: application to the seismic response problem, Geophys. J. Int. , **99**, 321-329.

Sochacki, J. S. , George J. H., et al. , 1991, Interface conditions for acoustic and elastic wave propagation, Geophysics, **56**, 168-181.

Stephen, R. A. , 1983, A comparison of finite difference and reflectivity seismograms for marine models, Geophys. J. Roy. Astr. Soc. , **72**, 39-58.

Tsingas, C. , Vafidis, A. , and Kanasewich, E. R. , 1990, Elastic wave propagation in transversely isotropic media using finite difference method, Geophys. Prosp. , **38**, 933-949.

Virieux, J. , 1986, P-SV wave propagation in heterogeneous media: velocity-stress finite-difference method, Geophysics, **51**, 889-901.

Zahradnik, J. , 1985, Programs for computing and analyzing SH wave fields in two-dimensional absorbing block structures, In programs for interpreting seismic observations, N. N. Mateveeva(Editor), Naula, Lennigrad, **3**, 124-186.

Zahradnik, J. , and Hron F., 1987, seismic ground motion of sedimentary valleys: example La Molina, Lima, Peru, J. Geophys. , **62**, 31-37.

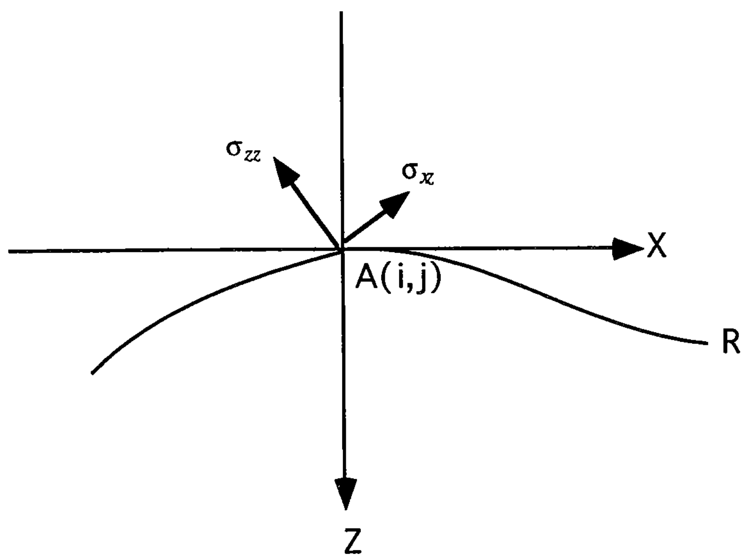

Fig. 1 Sketch map of the curved interior interface R.

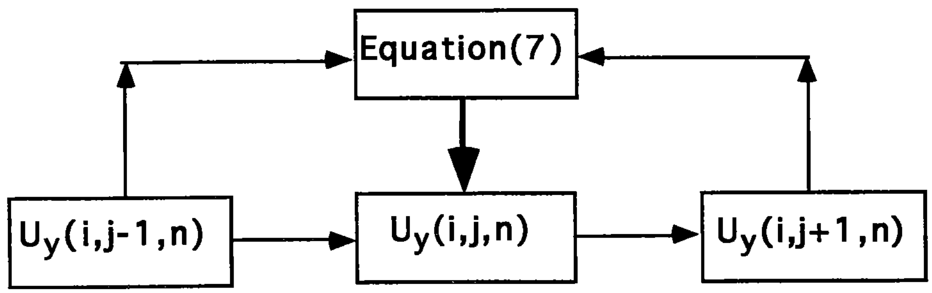

(a)

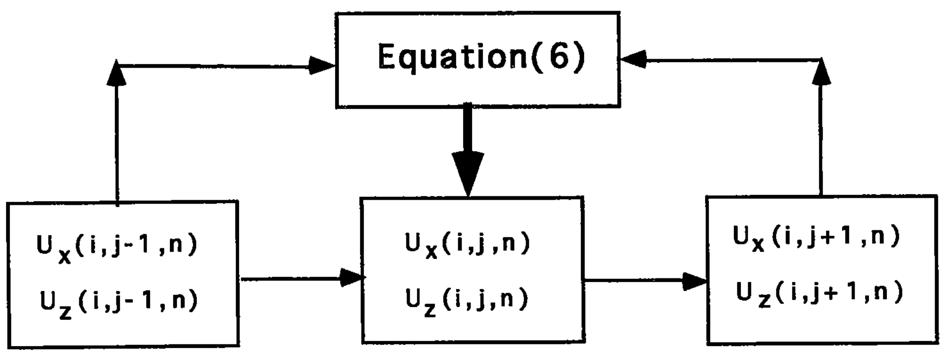

(b)

Fig. 2 Flowchart of FBI technique: (a) for y-component; (b) for x- and z-components.

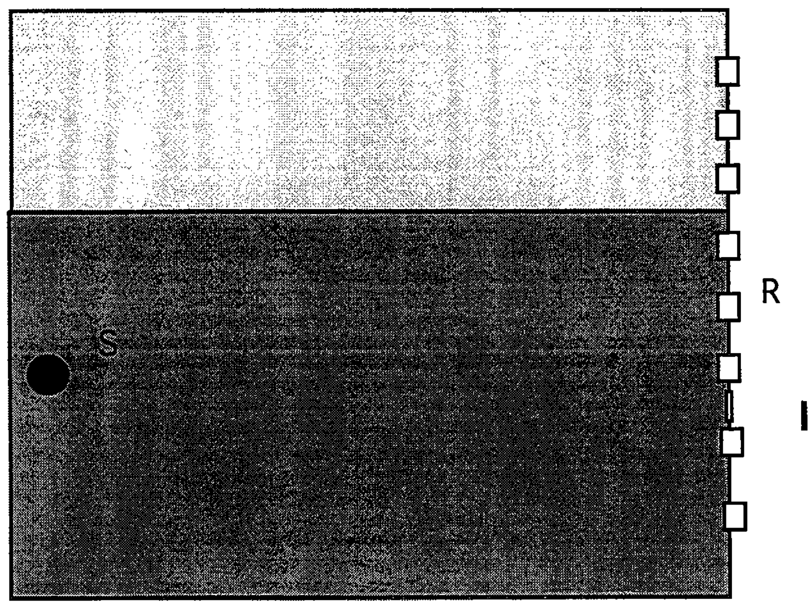

Fig. 3 Two-layer media model. S-Source, R-receiver.

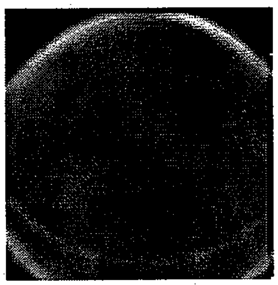

Fig. 4a

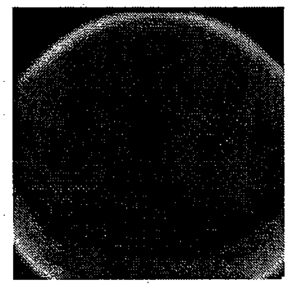

Fig. 5a

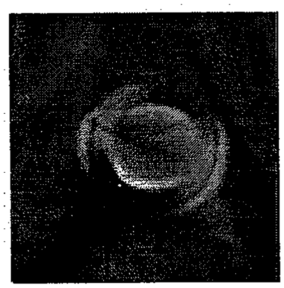

Fig. 4b

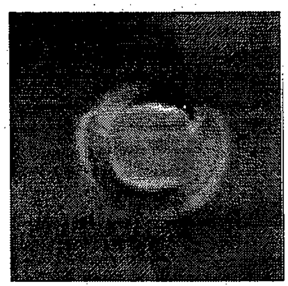

Fig. 5b

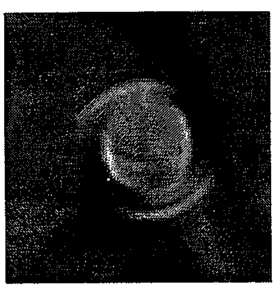

Fig. 4c

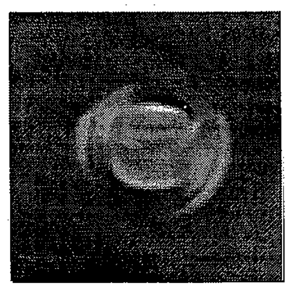

Fig. 5c

Fig. 6a

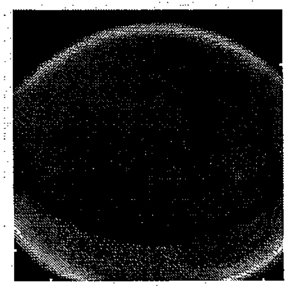

Fig. 7a

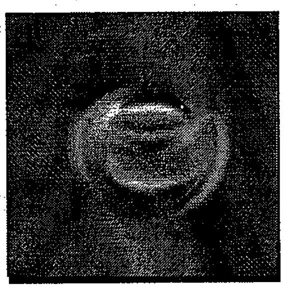

Fig. 6b

Fig. 7b

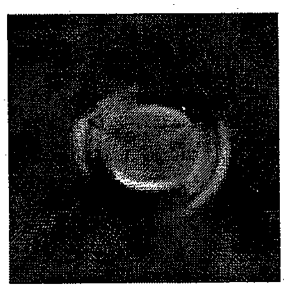

Fig. 6c

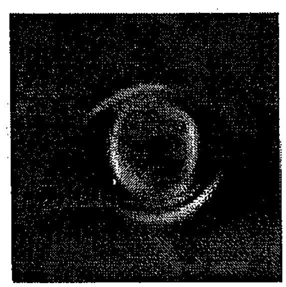

Fig. 7c